JCTC Journal of Chemical Theory and Computation

Multireference Model Chemistries for Thermochemical Kinetics

Oksana Tishchenko,* Jingjing Zheng, and Donald G. Truhlar*

Department of Chemistry and Supercomputing Institute, University of Minnesota, Minneapolis, Minnesota 55455-0431

Received March 5, 2008

Abstract: By combining the generalized valence bond ansatz of correlated participating orbitals (CPO) with the complete-active-space prescription for selecting configurations and with the use of multireference second order perturbation theory (MRMP2) for including dynamical correlation, we define three levels of multireference (MR) theoretical model chemistries for electronic structure calculations of chemical reaction energies and barrier heights. The three levels differ in their choice of which orbitals are considered to be participating; the choices are called nominal (*nom*-CPO), moderate (*mod*-CPO), and extended (*ext*-CPO). Combining any of these three choices with a method for treatment of dynamical correlation energy and a one-electron basis set yields a theoretical model chemistry. Unlike the full-valence choice of active orbitals, the CPO choices lead to active spaces that contain the orbitals needed to include important static correlation effects on chemical reactions but do not increase with the size of the nonparticipating portion of the system, and hence they remain viable computational options even for many large and complex reacting systems. The accuracies of the new levels, combined with the MG3S basis set (a partially augmented, multiply polarized valence triple-ζ basis with appropriately tight *d* functions for 3*p*-block elements) and with the fully augmented correlation-consistent aug-cc-pVTZ basis set, are assessed against a previously presented database of barrier heights for diverse reaction types. We find that *nom*-CPO level captures the bulk of the static correlation energy, and MRMP2/*nom*-CPO calculations have an average error of only 1.4 kcal/mol in barrier heights, which may be compared to 5.0 kcal/mol for single-reference MP2 theory, 2.5 kcal/mol for CCSD, and 4.1 and 1.0 kcal/mol for the B3LYP and M06−2X density functionals, respectively. The accuracy of MRMP2/CPO for transition structure bond lengths and donor−acceptor distances is excellent, with a mean unsigned error of only 0.007 Å as compared to 0.018 Å for CCSD, 0.019 Å for M06−2X, and 0.039 Å for MP2 and B3LYP. We also introduce a new multireference diagnostic, called the *M* diagnostic, that allows one to measure the importance of static correlation in a given reagent or transition state.

1. Introduction

The concept of theoretical model chemistry[1–4] is central to much recent progress in computational chemistry. A theoretical model chemistry is "an approximate but well-defined mathematical procedure of simulation".[2] Examples of popular theoretical model chemistries include HF/4−31G,[5] MP3/6−31G(d),[6] AM1,[7] B3LYP/6−31G(d),[8] Weizmann-1,[9] G3S,[10] MPW1K/6−31+G(d,p),[11] MR-G2(MP2),[12] BMC-CCSD,[13] ROCBS-QB3,[14] and innumerable others. With few exceptions,[12] essentially all theoretical model chemistries that are based on wave functions involve single-reference methods, that is, they are post-Hartree−Fock correlation methods based on a single-configuration reference state. Multireference methods, which are based on a multiconfiguration reference state, can provide increased accuracy for treating

* Corresponding author e-mail: truhlar@umn.edu (D.G.T.), o_t@t1.chem.umn.edu (O.T.).

10.1021/ct800077r CCC: $40.75
Published on Web 07/01/2008

many open-shell systems and transition states, especially when excited configurations are nearly degenerate with the ground state.[15] However, multireference methods have not been widely used as theoretical model chemistries and have been difficult to test systematically because the best choice of a reference state is system dependent; thus the precise reference state to be used for simulating a given process is not well defined by the method. The goals of the present article are, first, to define, in a general way, three levels of reference states suitable for calculating transition states, and, second, to test multireference calculations based on these reference states against a representative database[16] of diverse barrier heights.

The three levels of reference states that we define are complete active space self-consistent-field (CASSCF)[17–21] (equivalent to the fully optimized reaction space (FORS))[22] wave functions with three different schemes for choosing the number of active electrons and the number of active orbitals. (Note that the CAS and FORS prescriptions then specify inclusion of all configuration state functions that can be created by various ways of occupying these orbitals.) The three theoretical model chemistries that we consider are all multireference Møller−Plesset second order perturbation theory[23,24] (MRMP2) based on the CASSCF reference states. The CASSCF wave function includes static correlation, with the precise amount included depending on the choice of active space, that is, on the choice of active orbitals and the number of active electrons; the perturbation treatment includes dynamical correlation energy to second order. For a given active space the performance of MRMP2 should be very similar to that of other perturbation methods based on CASSCF, such as CASPT2[25] and various other versions of multireference second order perturbation theory.[26,27] One could imagine also using the three levels of reference states that we define here with post-CASSCF methods that include dynamical correlation to a higher order, such as multireference configuration interaction theory[28,29] or multireference coupled cluster theory;[30–44] however, we will not pursue this here.

2. Multireference Model Chemistries

A CASSCF wave function is a complete-active-space configuration interaction (CASCI) wave function in which all orbitals and all configurational coefficients are simultaneously optimized. A CASCI wave function is one in which a set of "inactive" orbitals are doubly occupied in all configurations and the remaining n electrons are distributed in all possible ways, consistent with a given symmetry and spin, over a set of m "active" orbitals. For singlet states with $m = n/2$, CASSCF reduces to single-configuration Hartree−Fock, but as n and m increase with $m > n/2$, the number of configurations increases rapidly. For example, with (n/m) denoting n active electrons distributed over m active orbitals, the number of determinants in singlet (10/14), (14/14), and (14/15) calculations are[45] 1.0×10^6, 1.2×10^7, and 4.1×10^7, respectively, which puts such calculations near the limit of doability.

One scheme for selecting n and m is to set n equal to the number of valence electrons and m equal to the number of valence orbitals (e.g., the number of valence orbitals is 1 for H and 4 for B through Ne or for Al through Ar).[12,22] This is called a full-valence CAS,[46,47] and it is unaffordable for all but the smallest molecules. (For example, a full-valence CAS for propane is (20,20).) In addition, it is not necessarily the best strategy. Consider formic acid, for which a full-valence CAS is (18,14). This yields only five unoccupied orbitals to correlate nine doubly occupied orbitals. In generalized valence bond (GVB) theory, one needs one correlating orbital to correlate each doubly occupied orbital, and no correlating orbital is required for a singly occupied orbital.[48] (Note that when we call an orbital singly or doubly occupied or unoccupied, we refer to its occupancy in the dominant configuration. Since all distributions of active electrons among active orbitals are included in the configuration list, any orbital in the active space is typically doubly occupied in some configurations and singly occupied or unoccupied in others).

Based on experience and the GVB analogy, we adopt the following guiding principle: To properly correlate the orbitals in the active space, there should be one correlating (i.e., unoccupied) orbital for every doubly occupied orbital in the active space. Furthermore, to keep the size of the active space manageable, we adopt another principle: only the orbitals that participate most strongly in bond breaking and bond forming are included in the active space. The combination of these two principles is called the correlated participating orbitals (CPO) scheme.

We will identify three choices of CPO, based on how we define participating orbitals: nominal (*nom*-CPO), moderate (*mod*-CPO), and extended (*ext*-CPO). In *nom*-CPO, the participating orbitals are those that describe bonds that break or form during the reaction. In *mod*-CPO, the participating orbitals are the nominal ones plus unshared pairs in p orbitals geminal to bonds that are broken or formed. In *ext*-CPO, the participating orbitals are the moderate ones plus unshared pairs in s orbitals or hybrid orbitals that are geminal to bonds being broken or formed. (Although the orbitals are delocalized, no confusion arises with identifying the most strongly bound lone pairs with s orbitals and the less strongly bound ones with p orbitals; this is commonly used[49] language.) Thus definitions of the three levels may be more clear when we give examples below.

For participating orbitals that are σ or π bonding orbitals, we take the correlating orbitals to be the corresponding σ^* and π^* antibonding orbitals, respectively. For participating orbitals that are $2p$ lone pairs, the correlating orbital is a $2p'$ orbital: $2p'_x$ for $2p_x$, $2p'_y$ for $2p_y$, and $2p'_z$ for $2p_z$. (In this notation, an orbital with a prime indicates an orbital that occupies approximately the same space as the corresponding orbital without a prime.) For $3p$ lone pairs, we use molecular orbitals of mixed $3p'/d$ character, one for each $3p$ orbital. (These are simply labeled $3d$ in Table 1.) For participating orbitals that are $2s$ lone pairs, the correlating orbital is a $2s'$ orbital. For participating orbitals with $3s$ lone pair characters, we make an exception to the 1:1 rule, and we add any $3d$ orbitals that have not already been added. We use $3d$ orbitals rather than $3s'$ because the latter are much higher in energy.

The key point is that one uses a small number of reaction-specific orbitals that gradually transform from reactants to products and result in a smooth potential energy profile. Variationally optimizing a CASSCF wave function with a CPO scheme for prescription of the choice of active orbitals will not necessarily lead to the global minimum of the energy functional at all molecular geometries. Consider a unimolecular dissociation reaction in which a single bond is broken, that is, X-A → X + A. At those geometries where the X-A distance is significantly stretched, using the σ and σ^* orbitals of the bond being broken as the active orbitals (i.e., using the *nom*-CPO recipe) will likely lead to the global minimum of the CASSCF energy; however, at geometries close to the equilibrium geometry of the X-A bond, it most likely will not, especially if one or both molecular fragments involves π-bonds or unshared electron pairs. Therefore, care must be taken to make sure that one gets the orbitals corresponding to the chosen CPO scheme at all molecular geometries of interest; this can often be accomplished by using an appropriate initial orbital set for the SCF process. It is important to ensure that SCF process converges to orbitals that make the calculated potential energy surface continuous with continuous derivatives.

In this article we apply the CPO levels to the reactions of the DBH24 database. DBH24[16] is a representative[50] database of 24 barrier heights, consisting of the forward and reverse barrier heights ($V_f^{\ddagger}$ and $V_r^{\ddagger}$, respectively) of 12 diverse reactions. There are also 12 energies of reaction (ΔV) for these reactions. These are all defined to be zero-point exclusive; that is that they refer to differences in potential energy, not to 0 K enthalpies. In the present article, all 12 reactions are written in the exoergic or ergoneutral direction; thus $\Delta V \leq 0$, and $V_f^{\ddagger} \leq V_r^{\ddagger}$.

The present MRPT2 calculations are all nonrelativistic, but the experimental results include spin−orbit coupling, which is a relativistic effect. Thus we added the spin−orbit energy to all reagents for which it is nonzero; these values are (in kcal/mol): OH, −0.20;[51a] SH, −0.54;[51a] Cl, −0.84;[51b] thus they lower the energies of these open-shell species. The spin−orbit energies are assumed to be negligible at the saddle points, which is a general effect (for many reactions like those considered here) discussed elsewhere.[51c] All results in this article already have the nonzero spin−orbit energies of OH, SH, and Cl included.

The three levels of reference wave function yielded by the prescriptions for the three CPO choices are completely specified for the reactions in DBH24 in Table 1. This table also lists the number N_d of determinants for each case. In Table 1, the z axis coincides with the bond that breaks, and the x axis is perpendicular to the plane defined by the three nuclei that are the reaction centers (in each reaction **R1**-**R12** the three reaction centers can be identified as the key atoms that are involved in bond breaking and bond formation, e.g. O, H_t, C in **R1**, H, H_t, O in **R2**, H, H_t, S in **R3**, etc., where H_t denotes the transferred hydrogen). In definitions of participating orbitals in this table, a pipe is used to indicate an orbital at the reactant (left) and the corresponding orbital at the product (right) (only for the orbitals that change their characters during a reaction).

Reactions **R1**-**R3** are hydrogen transfer reactions; the *nom*-CPO active space for these reactions involves the bonding and antibonding orbitals for the bond that undergoes breaking/formation and the SOMO(s). Reactions **R5** and **R6** are heavy atom transfer reactions; the *nom*-CPO active space for for these reactions is constructed in the same way as for reactions **R1**-**R3**. Reactions **R7**-**R9** are S_N2 reactions of the $X^- + CH_3Y \rightarrow XCH_3 + Y^-$ type; the *nom*-CPO active space for these reactions involves the bond that undergoes breaking/formation, the orbital χ at an X/Y group with the unshared pair of electrons that donates/accepts the electrons, and a correlating orbital for the orbital χ; this correlating orbital is either a $2p'$ orbital (if χ is on a second-row atom) or a $3d_{z^2}$ orbital (if χ is on a third-row atom). Reactions **R10** and **R11** can be considered as either dissociation or addition reactions; the *nom*-CPO active space for these reactions consists of the bonding and antibonding orbital pair that describe the bond that undergoes breaking/formation (π_{NN}/σ_{NH} and π_{CC}/σ_{CH}) and the SOMO ($1s_H$). Reactions **R4** and **R12** involve a change of several bonds in the same reaction step; therefore, the *nom*-CPO active space is larger in these cases: in the case of **R4** it involves the $1s_H$ and all $2p_O$ and $2p_N$ orbitals and is the same as the *mod*-CPO active space; in the case of **R12** it involves the $1s_H$, $2s_N$, $2s_C$, $2p_N$, and $2p_C$ orbitals and is the same as the *mod*-CPO and *ext*-CPO active spaces.

3. Computational Details

Molecular orbitals were optimized by using multiconfigurational self-consistent field wave functions of the fully optimized reaction space FORS[22] type which is equivalent to CASSCF.[17–21] Dynamical electron correlation was included by using multireference second-order Møller−Plesset theory (MRMP2).[23,24] In MRMP2 calculations, all orbitals were correlated except the $1s$ orbitals on nonhydrogenic atoms. Molecular geometries of the reactants, products, and reaction saddle points were optimized using numerical MRMP2 gradients. When optimizing geometries of reactants or products we set them at least 25 Å apart.

nom-CPO calculations were carried out with two basis sets: the larger aug-cc-pVTZ basis[52,53] and the efficient MG3S basis.[54] MG3S is the same as 6-311+G(3*d*2*f*,2*df*,2*p*)[55] for H−Si and is of similar size but improved[56] for P−Ar. The sizes of these basis sets for the transition states in DBH24 are tabulated elsewhere;[57] the average numbers of basis functions for the transition states in DBH24 are 158 primitive Gaussians and 108 contracted functions for MG3S and 228 primitive functions and 165 contracted functions for aug-cc-pVTZ. For all levels of theory other than *nom*-CPO we employed the MG3S basis.

All multireference calculations were performed using GAMESS[58] codes, and all single-reference calculations were performed using *Gaussian*.[59] M05 and M06 calculations were performed with MN-GFM.[60]

4. Results

Tables 2, 3, and 4 give results for, respectively, the MRMP2/*nom*-CPO, MRMP2/*mod*-CPO, and MRMP2/*ext*-CPO model chemistries. $\Delta(V_f^{\ddagger})$ is the error in the forward barrier height, $\Delta(V_r^{\ddagger})$ is the error in the reverse barrier height, and $\Delta(\Delta V)$

Table 1. Active Orbitals and the Number of Determinants (N_d) in FORS/CASSCF Wave Functions for Reactions in DBH24

	nom-CPO		*mod*-CPO		*ext*-CPO	
reaction	MOs	N_d, n/m	MOs	N_d, n/m	MOs	N_d, n/m
R1: OH + CH_4 → CH_3 + H_2O	$\sigma_{OH}\|\sigma_{CH}$, $\sigma^*_{OH}\|\sigma^*_{CH}$, $2p_{zO}\|2p_{zC}$ (SOMO)	9 3/3	σ_{OH}, σ^*_{OH}, $2p_{zO}\|2p_{zC}$ (SOMO) $2p_{xO}$, $2p_{yO}$, $2p'_{xO}$, $2p'_{yO}$	1225 7/7	σ_{OH}, σ^*_{OH}, $2p_{zO}\|2p_{zC}$ (SOMO) $2p_{xO}$, $2p_{yO}$, $2p'_{xO}$, $2p'_{yO}$, $2s_O$, $2s'_O$	15876 9/9
R2: H + OH → O + H_2	$\sigma_{OH}\|\sigma_{HH}$, $\sigma^*_{OH}\|\sigma^*_{HH}$, $2p_{xO}$ (SOMO), $1s_H\|2p_{zO}$ (SOMO)	16 4/4	$\sigma_{OH}\|\sigma_{HH}$, $\sigma^*_{OH}\|\sigma^*_{HH}$, $2p_{xO}$ (SOMO), $1s_H\|2p_{zO}$ (SOMO), $2p_{yO}$,$2p'_{yO}$	225 6/6	$\sigma_{OH}\|\sigma_{HH}$, $\sigma^*_{OH}\|\sigma^*_{HH}$, $2p_{xO}$ (SOMO), $1s_H\|2p_{zO}$ (SOMO), $2p_{yO}$,$2p'_{yO}$, $2s'_O$, $2s_O$	3136 8/8
R3: H + H_2S → H_2 + HS	$\sigma_{SH}\|\sigma_{HH}$, $\sigma^*_{SH}\|\sigma^*_{HH}$, $1s_H\|3p_{zS}$ (SOMO)	9 3/3	$\sigma_{SH}\|\sigma_{HH}$, $\sigma^*_{SH}\|\sigma^*_{HH}$, $1s_H\|3p_{zS}$ (SOMO) $3p_{xS}$, $3p_{yS}$, $3d_{xyS}$, $3d_{y^2S}$	1225 7/7	$\sigma_{SH}\|\sigma_{HH}$, $\sigma^*_{SH}\|\sigma^*_{HH}$, $1s_H\|3p_{zS}$ (SOMO) $3p_{xS}$, $3p_{yS}$, $3d_{xyS}$, $3d_{y^2S}$, $3s_S$, $3d_{xzS}$, $3d_{yzS}$, $3d_{(x^2-z^2)S}$	152460 9/11
R4: H + N_2O → OH + N_2	$2p_{xO}$, $2p_{yO}$, $2p_{xN_a}$, $2p_{yN_a}$, $2p_{xN_b}$, $2p_{yN_b}$, $2p'_{xO}$, $2p'_yO$, $1s_H\|2p_{zO}$ (SOMO), $\sigma_{NO}\|\sigma_{NN}$, σ^*_{NO},$\|\sigma^*_{NN}$	213444 11/11	$2p_{xO}$, $2p_{yO}$, $2p_{xN_a}$, $2p_{yN_a}$, $2p_{xN_b}$, $2p_{yN_b}$, $2p'_{x}O$, $2p'_{yO}$, $1s_H\|2p_{zO}$ (SOMO), $\sigma_{NO}\|\sigma_{NN}$, σ^*_{NO},$\|\sigma^*_{NN}$	213444 11/11	$2p_{xO}$, $2p_{yO}$, $2p_{xN_a}$, $2p_{yN_a}$, $2p_{xN_b}$, $2p_{yN_b}$, $2p'_{xO}$, $2p'_{yO}$, $1s_H\|2p_{zO}$ (SOMO), $\sigma_{NO}\|\sigma_{NN}$, σ^*_{NO},$\|\sigma^*_{NN}$, $2s_{N_a}$, $2s_{N_b}$, $2s_O$, $2s'_{N_a}$, $2s'_{N_b}$, $2s'_O$	213444 11/11
R5: H + ClH → HCl + H	σ_{ClH}, σ^*_{ClH}, $1s_H$	9 3/3	σ_{ClH}, σ^*_{ClH}, $1s_H$, $3p_{yCl}$, $3d_{xyCl}$, $3d_{(x^2-y^2)Cl}$	1225 7/7	σ_{ClH}, σ^*_{ClH}, $1s_H$, $3s_{Cl}$, $3p_{xCl}$, $3p_{yCl}$, $3d_{xyCl}$, $3d_{(x^2-y^2)Cl}$ $3d_{xzCl}$, $3d_{yzCl}$, $3d_{z^2Cl}$	152460 9/11
R6: CH_3 + FCl → CH_3F + Cl	$\sigma_{FCl}\|\sigma_{CF}$, σ^*_{FCl},$\|\sigma^*_{CF}$, $2p_{zC}\|3p_{zCl}$ (SOMO)	9 3/3	$\sigma_{FCl}\|\sigma_{CF}$, σ^*_{FCl},$\|\sigma^*_{CF}$, $2p_{zC}\|3p_{zCl}$ (SOMO), $2p_{xF}$, $2p_{yF}$, $2p'_{xF}$, $2p'_{yF}$, $3p_{xCl}$, $3p_{yCl}$, $3d_{xyCl}$, $3d_{(x^2-y^2)Cl}$	213444 11/11	$\sigma_{FCl}\|\sigma_{CF}$, σ^*_{FCl},$\|\sigma^*_{CF}$, $2p_{zC}\|3p_{zCl}$ (SOMO), $2p_{xF}$, $2p_{yF}$, $2p'_{xF}$, $2p'_{yF}$, $3p_{xCl}$, $3p_{yCl}$, $3d_{xyCl}$, $3d_{(x^2-y^2)Cl}$, $2s_F$, $2's_F$, $3s_{Cl}$, $3d_{xzCl}$, $3d_{yzCl}$, $3d_{z^2Cl}$	472780880 15/17
R7: $Cl^-\cdots CH_3$ Cl → $ClCH_3\cdots Cl^-$	σ_{CCl}, σ^*_{CCl}, $3p_{zCl}$, $3d_{z^2Cl}$	36 4/4	σ_{CCl}, σ^*_{CCl}, $3p_{zCl}$, $3d_{z^2Cl}$, $3p_{xCla}$, $3p_{xClb}$, $3p_{yCla}$, $3p_{yClb}$, $3d_{xzCla}$, $3d_{xzClb}$, $3d_{yzCla}$, $3d_{yzClb}$	853776 12/12	σ_{CCl}, σ^*_{CCl}, $3p_{zCl}$, $3p_{xCla}$, $3p_{xClb}$, $3p_{yCla}$, $3p_{yClb}$, $3s_{Cla}$, $3s_{Clb}$, + 10 × d_{Cl}	5712638724 16/19
R8: $F^-\cdots CH_3Cl$ → $FCH_3\cdots Cl^-$	$\sigma_{CCl}\|\sigma_{CF}$, $\sigma^*_{CCl}\|\sigma^*_{CF}$, $2p_{zF}\|3p_{zCl}$, $3p_{zF}\|3d_{z^2Cl}$	36 4/4	$\sigma_{CCl}\|\sigma_{CF}$, $\sigma^*_{CCl}\|\sigma^*_{CF}$, $2p_{zF}\|3p_{zCl}$, $3p_{zF}\|3d_{z^2Cl}$, $3p_{xCl}$, $2p_{xF}$, $3p_{yCl}$, $2p_{yF}$, $3d_{xzCl}$, $2p'_{xF}$, $3d_{yzCl}$, $2p'_{yF}$	853776 12/12	$\sigma_{CCl}\|\sigma_{CF}$, $\sigma^*_{CCl}\|\sigma^*_{CF}$, $2p_{zF}\|3p_{zCl}$, $3p_{zF}\|3d_{z^2Cl}$, $3p_{xCl}$, $2p_{xF}$, $3p_{yCl}$, $2p_{yF}$, $3d_{xzCl}$, $2p'_{xF}$, $3d_{yzCl}$, $2p'_{yF}$ $2s_F$, $3s_{Cl}$, $3s_F$, $3d_{xyCl}$, $3d_{(x^2-y^2)Cl}$	590976100 16/17
R9: OH^- + CH_3F → $HOCH_3$ + F^-	$\sigma_{CF}\|\sigma_{CO}$, $\sigma^*_{CF}\|\sigma^*_{CO}$, $2p_{zO}\|2p_{zF}$, $2p'_{zO}\|2p'_{zF}$	36 4/4	$\sigma_{CF}\|\sigma_{CO}$, $\sigma^*_{CF}\|\sigma^*_{CO}$, $2p_{zO}\|2p_{zF}$, $2p'_{zO}\|2p'_{zF}$, $2p_{xF}$, $2p_{yF}$, $2p_{xO}$, $2p_{yO}$, $2p_{x'F}$, $2p_{y'F}$, $2p_{x'O}$, $2p_{y'O}$	853776 12/12	$\sigma_{CF}\|\sigma_{CO}$, $\sigma^*_{CF}\|\sigma^*_{CO}$, $2p_{zO}\|2p_{zF}$, $2p'_{zO}\|2p'_{zF}$ $2p_{xF}$, $2p_{yF}$, $2p_{xO}$, $2p_{yO}$, $2p_{x'F}$, $2p_{y'F}$, $2p_{x'O}$, $2p_{y'O}$ $2s_F$, $2s_O$, $2s'_F$, $2s'_O$	165636900 16/16
R10: H + N_2 → HN_2	$2p_{zNa}\|\sigma_{NH}$, $2p_{zNb}$, $1s_H\|\sigma^*_{NH}$	9 3/3	$2p_{zNa}\|\sigma_{NH}$, $2p_{zNb}$, $1s_H\|\sigma^*_{NH}$ $2\pi_{xNN}$, $2\pi_{yNN}$, $2\pi_x{}^*_{NN}$, $2\pi_y{}^*_{NN}$	1225 7/7	$2p_{zNa}\|\sigma_{NH}$, $2p_{zNb}$, $1s_H\|\sigma^*_{NH}$ $2\pi_{xNN}$, $2\pi_{yNN}$, $2\pi_x{}^*_{NN}$, $2\pi_y{}^*_{NN}$ $2s_{Na}$, $2s_{Nb}$, $3s_{Na}$, $3s_{Na}$	213444 11/11
R11: H + C_2H_4 → CH_3CH_2	$2p_{zCa}\|\sigma_{CH}$, $2p_{zCb}$, $1s_H\|\sigma^*_{CH}$	9 3/3	$2p_{zCa}\|\sigma_{CH}$, $2p_{zCb}$, $1s_H\|\sigma^*_{CH}$	9 3/3	$2p_{zCa}\|\sigma_{CH}$, $2p_{zCb}$, $1s_H\|\sigma^*_{CH}$	9 3/3
R12: HCN → HNC	$\sigma_{CH}\|\sigma_{NH}$, $\sigma^*_{CH}\|\sigma^*_{NH}$ $2p_{xC}$, $2p_{yC}$, $2p_{xN}$, $2p_{yN}$, $2p'_{xC}$, $2p'_{yC}$, $2p'_{xN}$, $2p'_{yN}$	63504 10/10	$\sigma_{CH}\|\sigma_{NH}$, $\sigma^*_{CH}\|\sigma^*_{NH}$, $2p_{xC}$, $2p_{yC}$, $2p_{xN}$, $2p_{yN}$, $2p'_{xC}$, $2p'_{yC}$, $2p'_{xN}$, $2p'_{yN}$	63504 10/10	$\sigma_{CH}\|\sigma_{NH}$, $\sigma^*_{CH}\|\sigma^*_{NH}$, $2p_{xC}$, $2p_{yC}$, $2p_{xN}$, $2p_{yN}$, $2p'_{xC}$, $2p'_{yC}$, $2p'_{xN}$, $2p'_{yN}$	63504 10/10

is the error in the energy of reaction. Tables 5 and 6 give results for, respectively, single-reference Møller−Plesset second-order perturbation theory[61] (MP2) and coupled cluster theory with single and double excitations[62] (CCSD), respectively. The MP2 and CCSD calculations for open-shell cases are based on unrestricted Hartree−Fock reference functions. All results in Tables 2–6 correspond to consistently optimized structures at the level specified (the present article contains no single-point energies).

Note that in some cases, namely **R4**, **R11**, and **R12**, the model chemistry definitions yield the same size active space for *nom*-CPO and *mod*-CPO. In the case of **R12**, the active

Table 2. Barrier Heights and Errors for Reactions in DBH24 Calculated with MRMP2/*nom*-CPO with MG3S and aug-cc-pVTZ Basis Sets

reaction	(*n*/*m*)	$V_f^{\ddagger}$	$V_f^{\ddagger}$ (best est)	$V_r^{\ddagger}$	$V_r^{\ddagger}$ (best est)	$\Delta(V_f^{\ddagger})$	$\Delta(V_r^{\ddagger})$	$\Delta(\Delta V)$
			MG3S					
R1: OH + CH_4 → CH_3 + H_2O	(3/3)	6.23	6.7	20.87	19.6	−0.5	1.3	−1.7
R2: H + OH → O + H_2	(4/4)	10.6	10.7	14.78	13.1	−0.1	1.7	−1.8
R3: H + H_2S → H_2 + HS	(3/3)	3.31	3.6	22.85	17.3	−0.3	5.6	−5.8
R4: H + N_2O → OH + N_2	(11/11)	18.83	18.1	80.12	83.2	0.7	−3.1	3.8
R5: H + ClH → HCl + H	(3/3)	16.24	18.0	16.24	18.0	−1.8	−1.8	0.0
R6: CH_3 + FCl → CH_3F + Cl	(3/3)	4.56	7.4	61.49	60.5	−2.9	1.0	−3.8
R7: $Cl^-\cdots CH_3Cl$ → $ClCH_3\cdots Cl^-$	(4/4)	14.64	13.6	14.64	13.6	1.0	1.0	0.0
R8: $F^-\cdots CH_3Cl$ → FCH_3+ Cl^-	(4/4)	3.29	2.9	30.10	29.6	0.4	0.5	−0.1
R9: OH^- + CH_3F→ $HOCH_3\cdots F^-$	(4/4)	−1.13	−2.8	18.38	17.3	1.7	1.1	0.6
R10: HN_2 → H + N_2	(3/3)	14.96	14.7	9.61	10.7	0.3	−1.1	1.4
R11: H + C_2H_4 → CH_3CH_2	(3/3)	2.44	1.7	39.07	41.8	0.7	−2.7	3.4
R12: HNC → HCN	(10/10)	32.14	33.1	48.74	48.2	−1.0	0.6	−1.5
MUE(DBH24)						0.9	1.8	2.0
MUE(DBHS22)						1.0	1.6	1.8
MUE(DBHS20)						1.0	1.9	2.4
MUE(DBHS12)						0.5	2.1	2.6
			aug-cc-pVTZ					
R1: OH + CH_4 → CH_3 + H_2O	(3/3)	5.63	6.7	20.40	19.6	1.1	−0.8	−1.9
R2: H + OH → O + H_2	(4/4)	9.75	10.7	13.70	13.1	0.9	−0.6	−1.6
R3: H + H_2S → H_2 + HS	(3/3)	2.13	3.6	20.23	17.3	1.5	−2.9	−4.4
R5: H + ClH → HCl + H	(3/3)	14.75	18.0	14.75	18.0	3.3	3.3	0.0
R6: CH_3 + FCl → CH_3F + Cl	(3/3)	3.93	7.4	58.95	61.0	3.5	2.1	−1.4
R7: $Cl^-\cdots CH_3Cl$ → $ClCH_3\cdots Cl^-$	(4/4)	13.42	13.6	13.42	13.6	0.2	0.2	0.0
R8: $F^-\cdots CH_3Cl$ → $FCH_3\cdots Cl^-$	(4/4)	3.68	2.9	25.88	29.6	−1.1	3.8	4.9
R9: OH^- + CH_3F→ $HOCH_3$ + F^-	(4/4)	−1.78	−2.8	16.64	17.3	−1.7	−1.0	0.7
R10: HN_2 → H + N_2	(3/3)	9.80	10.7	13.58	14.7	0.9	1.1	0.2
R11: H + C_2H_4 → CH_3CH_2	(3/3)	1.67	1.7	39.78	41.8	0.1	2.0	1.9
R12: HNC → HCl	(10/10)	31.15	33.1	47.72	48.2	2.0	0.4	−1.5
MUE(DBHS22)						1.4	1.4	1.7
MUE(DBHS12)						1.1	1.3	1.9

Table 3. Barrier Heights and Errors for Reactions in DBH24 Calculated with MRMP2/*mod*-CPO/MG3S

reaction	(*n*/*m*)	$V_f^{\ddagger}$	$V_f^{\ddagger}$ (best est)	$V_r^{\ddagger}$	$V_r^{\ddagger}$ (best est)	$\Delta(V_f^{\ddagger})$	$\Delta(V_r^{\ddagger})$	$\Delta(\Delta V)$
R1: OH + CH_4 → CH_3 + H_2O	(7/7)	7.17	6.7	19.2	19.6	0.5	−0.4	0.9
R2: H + OH → O + H_2	(6/6)	10.61	10.7	16.18	13.1	−0.1	3.1	−3.2
R3: H + H_2S → H_2 + HS	(7/7)	4.33	3.6	21.49	17.3	0.7	4.2	−3.5
R4: H + N_2O → OH + N_2	(11/11)	18.83	18.1	79.92	83.2	0.7	−3.3	4.0
R5: H + ClH → HCl + H	(7/7)	18.78	18.00	18.78	18.0	0.8	0.8	0.0
R6: CH_3 + FCl → CH_3F + Cl	(11/11)	4.35	7.4	61.77	61.0	−3.1	0.8	−3.8
R9: OH^- + CH_3F → $HOCH_3\cdots F^-$	(12/12)	−0.04	−2.8	21.34	17.3	2.7	4.0	−1.3
R10: HN_2 → H + N_2	(7/7)	12.36	10.7	16.25	14.7	1.6	1.6	−0.1
R11: H + C_2H_4 → CH_3CH_2	(3/3)	2.44	1.7	39.07	41.8	0.7	−2.7	3.4
R12: HNC → HCN	(10/10)	32.14	33.1	48.74	48.2	−1.0	0.6	−1.6
MUE(DBHS20)						1.2	2.1	2.2
MUE(DBHS12)						0.8	2.1	2.1

Table 4. Barrier Heights and Errors for Reactions in DBH24 Calculated with MRMP2/*ext*-CPO/MG3S

reaction	(*n*/*m*)	$V_f^{\ddagger}$	$V_f^{\ddagger}$ (best est)	$V_r^{\ddagger}$	$V_r^{\ddagger}$ (best est)	$\Delta(V_f^{\ddagger})$	$\Delta(V_r^{\ddagger})$	$\Delta(\Delta V)$
R1: OH + CH_4 → CH_3 + H_2O	(9/9)	5.63	6.7	20.33	19.6	−1.1	0.7	−1.8
R2: H + OH → O + H_2	(8/8)	10.80	10.7	15.06	13.1	0.1	−2.0	−1.9
R3: H + H_2S → H_2 + HS	(9/11)	4.59	3.6	19.93	17.3	1.0	2.6	−1.6
R10: HN_2 → H + N_2	(11/11)	11.07	10.7	15.33	14.7	0.4	0.6	−0.3
R11: H + C_2H_4 → CH_3CH_2	(3/3)	2.44	1.7	39.07	41.8	0.7	−2.7	3.4
R12: HNC → HCN	(10/10)	32.14	33.1	48.74	48.2	−1.0	0.6	−1.5
MUE(DBHS12)						0.7	1.5	1.8

space is also the same size for *ext*-CPO. Note also that some of the larger calculations are omitted for *mod*-CPO and *ext*-CPO due to the large number of determinants or difficulty converging the geometry optimization, and one of the *nom*-CPO/aug-cc-pVTZ calculations is also omitted; thus the errors in these cases are for subsets of DBH24. These subsets are called DBHS22, DBHS20, and DBHS12, and these mean unsigned errors (MUEs) are also given for other methods (when available) for comparison. (Subset 22 (S22) is missing **R4**; subset 20 (S20) is missing **R7** and **R8**; and subset 12 (S12) is missing **R4**-**R9**.)

Tables 2–6 give separate MUEs for forward and reverse barrier heights as well as the MUEs for energies of reaction. The final MUE is the average over those for forward and reverse barriers, and these are given in Table 7.

5. Discussion

Before discussing the calculated barrier heights and energies of reaction, we analyze the extent of multireference character in the reagents and transition states. For this purpose we have defined a diagnostic quantity M in terms of the eigenvalues,

Table 5. Barrier Heights and Errors for Reactions in DBH24 Calculated with MP2/MG3S

reaction	$V_f^‡$	$V_f^‡$ (best est)	$V_r^‡$	$V_r^‡$ (best est)	$\Delta(V_f^‡)$	$\Delta(V_r^‡)$	$\Delta(\Delta V)$
R1: OH + CH_4 → CH_3 + H_2O	9.16	6.7	25.48	19.6	2.5	5.9	−3.4
R2: H + OH → O + H_2	18.50	10.7	17.47	13.1	7.8	4.4	3.4
R3: H + H_2S → H_2 + HS	7.72	3.6	18.81	17.3	4.1	−1.5	2.6
R4: H + N_2O → OH + N_2	36.25	18.1	87.57	83.2	18.1	4.4	13.8
R5: H + ClH → HCl + H	24.50	18.0	24.50	18.0	6.5	6.5	0.0
R6: CH_3 + FCl → CH_3F + Cl	15.82	7.4	72.94	61.0	8.4	11.9	−3.5
R7: $Cl^-\cdots CH_3Cl$ → $ClCH_3\cdots Cl^-$	14.46	13.6	14.46	13.6	0.9	0.9	0.0
R8: $F^-\cdots CH_3Cl$ → $FCH_3\cdots Cl^-$	3.75	2.9	31.19	29.6	0.9	1.6	−0.7
R9: OH^- + CH_3F → $HOCH_3$ + F^-	−2.84	−2.8	17.51	17.3	−0.1	0.2	−0.2
R10: HN_2 → H + N_2	9.89	10.7	28.04	14.7	−0.8	13.4	−14.2
R11: H + C_2H_4 → CH_3CH_2	9.93	1.7	46.04	41.8	8.2	4.3	3.9
R12: HNC → HCN	35.31	33.1	53.21	48.2	2.2	5.0	−2.9
MUE(DBH24)					5.0	5.0	4.1
MUE(DBHS22)					3.8	5.1	3.2
MUE(DBHS20)					5.9	5.7	4.8
MUE(DBHS12)					4.3	5.7	5.1

Table 6. Barrier Heights and Errors for Reactions in DBH24 Calculated with CCSD/MG3S

reaction	$V_f^‡$	$V_f^‡$ (best est)	$V_r^‡$	$V_r^‡$ (best est)	$\Delta(V_f^‡)$	$\Delta(V_r^‡)$	$\Delta(\Delta V)$
R1: OH + CH_4 → CH_3 + H_2O	9.94	6.7	21.19	19.6	3.2	1.6	1.6
R2: H + OH → O + H_2	11.36	10.7	16.96	13.1	0.7	3.9	−3.2
R3: H + H_2S → H_2 + HS	5.10	3.6	21.69	17.3	1.5	4.4	−2.9
R4: H + N_2O → OH + N_2	19.89	18.1	92.04	83.2	1.8	8.8	−7.1
R5: H + ClH → HCl + H	21.10	18.0	21.10	18.0	3.1	3.1	0.0
R6: CH_3 + FCl → CH_3F + Cl	9.29	7.4	67.10	61.0	1.9	6.1	−4.2
R7: $Cl^-\cdots CH_3Cl$ → $ClCH_3\cdots Cl^-$	14.94	13.6	14.94	13.6	1.3	1.3	0.0
R8: $F^-\cdots CH_3Cl$ → $FCH_3\cdots Cl^-$	3.64	2.9	34.09	29.6	0.7	4.5	−3.7
R9: OH^- + CH_3F → $HOCH_3$ + F^-	−0.90	−2.8	19.72	17.3	1.9	2.4	−0.5
R10: HN_2 → H + N_2	11.55	10.7	16.47	14.7	0.8	1.8	−0.9
R11: H + C_2H_4 → CH_3CH_2	3.09	1.7	44.02	41.8	1.4	2.3	−0.9
R12: HNC → HCN	34.33	33.1	48.89	48.2	1.2	0.7	0.5
MUE(DBH24)					1.6	3.4	2.1
MUE(DBHS22)					1.6	2.9	1.7
MUE(DBHS20)					1.7	3.5	2.2
MUE(DBHS12)					1.5	2.4	1.7

$n(i)$ or $n(j)$, of the first-order density matrix of the CASSCF wave functions. These eigenvalues are usually called the natural occupation numbers, and n(MCDONO), n(SOMO), and n(MCUNO) are respectively the natural orbital occupation numbers of the most correlated doubly occupied natural orbital (MCDONO), a singly occupied natural orbital (SOMO), and the most correlating unoccupied natural orbital (MCUNO). The MCDONO is defined as the "doubly occupied" (recall that this refers to the dominant configuration) natural orbital with the smallest $n(i)$, and the MCUNO is the "unoccupied" (again, in the dominant configuration) natural orbital with the largest occupation number. Let n_{SOMO} be the number of singly occupied molecular orbitals in the dominant configuration of the ground electronic state (label them $j = 1,..., n_{SOMO}$). Then the multireference diagnostic is defined as

$$M = \frac{1}{2}\left(2 - n(\mathrm{MCDONO}) + \sum_{j=1}^{n_{SOMO}} |n(j) - 1| + n(\mathrm{MCUNO})\right) \quad (1)$$

Note that one enumerates n_{SOMO} at a molecular geometry that represents a stationary structure on the potential energy surface, e.g., for dissociation of the hydrogen molecule, n_{SOMO} would be zero rather than two. Since $0 \le n(i \text{ or } j) \le 2$, the upper bound on the numerator is $2 + n_{SOMO}$, and therefore one must always have $0 \le M \le 1$ for closed-shell systems. For systems with open shells, the upper bound on M depends on n_{SOMO}, but since the occupancies of singly occupied natural orbitals are close to 1 (for reactions in DBH24, the largest deviation from unity is 0.011) and since we do not include a correlating orbital for SOMOs, the maximal value of M is not significantly larger than 1. For a Hartree−Fock wave function, M would be zero, and larger M for the CASSCF wave function shows larger static correlation.

For systems involving participating π bonds, such as, e.g., reaction **R11**, the MCDONO is often the same as the highest-energy molecular orbital (HOMO), and the MCUNO is the same as the lowest-energy unoccupied molecular orbital (LUMO), but this need not be the case in general.

In order to place the M values in perspective, it is interesting to compute M values for some prototype cases. Therefore, Figure 1 illustrates the manner in which the M values of the H_2, ethylene, and ozone molecules change as functions of the internuclear distances. The ozone molecule is a widely known example of the "multireference" system.[65] At the experimental equilibrium nuclear configurations of these molecules, the M values are 0.024, 0.072, and 0.225, respectively. As bonds stretch, the M value in the ozone case increases much more rapidly as compared to the other cases, and the M value for breaking a double bond increases more rapidly than that for breaking a single bond. Notice that the M value for C_2H_4 in Table 8 is 0.086, which is 19% larger than the 0.072 quoted above; there are two reasons for this difference. First of all, the value in Table 8 is for a geometry optimized at the MRMP2/*nom*-CPO/MG3S level, whereas Figure 1 is based on the experimental geometry which has a C−C bond length of 1.339 Å (vs 1.331 Å for Table 8).

Table 7. MUEs for MRMP2, MP2, and CCSD for Reactions in DBH24

method	MUE
DBH24	
MRMP2/*nom*-CPO/MG3S	1.4
MP2/MG3S	5.0
CCSD/MG3S	2.5
B3LYP/MG3S	4.1
M06−2X/MG3S	1.0
M05−2X/MG3S	1.7
DBHS22	
MRMP2/*nom*-CPO/MG3S	1.3
MRMP2/*nom*-CPO/aug-cc-pVTZ	1.4
MP2/MG3S	4.5
CCSD/MG3S	2.3
B3LYP/MG3S	3.8
M06−2X/MG3S	1.1
M05−2X/MG3S	1.6
DBHS20	
MRMP2/*nom*-CPO/MG3S	1.5
MRMP2/*mod*-CPO/MG3S	1.7
MP2/MG3S	5.8
CCSD/MG3S	2.6
B3LYP/MG3S	4.2
M06−2X/MG3S	1.0
M05−2X/MG3S	1.8
DBHS12	
MRMP2/*nom*-CPO/MG3S	1.3
MRMP2/*nom*-CPO/aug-cc-pVTZ	1.2
MRMP2/*mod*-CPO/MG3S	1.5
MRMP2/*ext*-CPO/MG3S	1.1
MP2/MG3S	5.0
CCSD/MG3S	2.0
B3LYP/MG3S	3.1
M06−2X/MG3S	1.2
M05−2X/MG3S	1.6

Second, and more important, is the dependence on the active space. The value in Table 8 is for reaction **R11**, for which the *nom*-CPO active space includes only the π and π^* orbitals for ethylene, but Figure 1 is for breaking a double bond, and so the active space includes σ_{CC} and σ^*_{CC} as well.

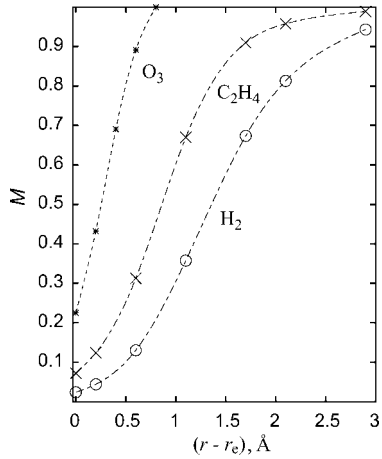

Figure 1. Mutlireference diagnostics *M* for H_2, ethylene, and ozone in their ground electronic states calculated with FORS(2/2), FORS(4/4), and FORS(12/12), respectively, as functions of the HH, CC stretching, and OO symmetric stretching coordinates, respectively. The equilibrium values of those distances that are varied are as follows: r_{eHH} = 0.741 Å,[63] r_{eCC} = 1.339 Å,[64] r_{eOO} = 1.278 Å.[64] The values of the other coordinates (held fixed) are r_{eCH} = 1.086 Å,[64] ∠HCH = 117.6°,[64] ∠HCC = 121.2°,[64] ∠OOO = 116.8°.[64]

Another interesting comparison is the reaction of H with H_2O_2 to give H_2O + OH or HO_2 + H_2. In a recent study[44] we found much greater multireference effects in the former than in the latter. Now we calculate *M* values of 0.099 and 0.064, respectively, for these reactions at the *mod*-CPO level. The fact that the former channel has a higher *M* value is consistent with our previous experience.

The multireference diagnostics for all CPO/MG3S calculations are given in Tables 8–10. Several interesting features emerge. First, all *M* values for reagents (a "reagent" is a reactant or product) are less than or equal to 0.086, and all *M* values for transition states are less than or equal to 0.106. Second, in all reactions except **R7** and **R8** and sometimes **R10**-**R12**, *M* is larger for the transition state than for either reagent. The average transition state *M* value is 0.054 for *nom*-CPO, 0.059 for *mod*-CPO, and 0.057 for *ext*-CPO. These are very consistent, especially consider that the latter two values are for subsets of the reactions. The chief exceptions to consistency of *M* from level to level are reaction **R6**, where *M* at the saddle point is surprisingly 0.03 lower at the higher *mod*-CPO level than at *nom*-CPO, and reaction **R10**, where *M* at the reactant is 0.05 lower at the *nom*-CPO than the average *M* at *mod*-CPO and *ext*-CPO levels. The differences in *M* for different levels for the cases with level dependence are due to two kinds of effects: (i) The MCDONO/MCUNO pair of the largest active spaces is not the same as the orbital that describes a breaking/forming bond; and thus this pair is "inactive" in the *nom*-CPO case, while it is "active" at higher *mod*-CPO and *ext*-CPO levels; in this case the *M* values for *nom*-CPO will be lower than those that at the higher levels (examples are the reactants in **R1**, **R3**, and **R10**). (ii) The inclusion of "extra" orbitals in *mod*-CPO and/or *ext*-CPO levels can result in a change of the natural orbital occupation numbers of the MCDONO and MCUNO; in this case the *M* values for *nom*-CPO can be either lower or higher than those that at the higher levels (the chief example is reaction **R6**).

Now we consider the energetics. Tables 2–4 show that the mean errors in MRMP2/CPO calculations are smaller for the forward (exothermic) reactions than for the reverse. This is reasonable since, by Hammond's postulate,[66] we expect the transition state of an exothermic reaction to resemble the reactants more than the products. Thus errors in dynamical correlation energies are more likely to cancel for this direction of reaction. Interestingly, the error in the MP2 barrier heights in Table 5 does not show this difference in accuracy between forward and reverse barrier heights. The comparison of MRMP2 to MP2 is particularly interesting in that they both correspond to second-order perturbation theory but with different reference states. Tables 2–5 and 7 show that the errors in MP2 barrier heights are, on average, about $3^1/_2$ times larger than those for any of the MRMP2/CPO model chemistries. One might expect MP2 to be relatively better for energies of reaction than for barrier heights because the reagents usually have smaller static correlation effects (as shown by the *M* values) than the transition states. This expectation is born out, but Tables 2–5 show that MP2 still has errors 2−3 times larger than MRMP2 even for energies of reaction.

Table 8. Mutlireference Diagnostics for Reactions in DBH24 Calculated with *nom*-CPO/MG3S

reaction	saddle point	reactants	products
R1: $OH + CH_4 \rightarrow CH_3 + H_2O$	0.025	0.018	0.021
R2: $H + OH \rightarrow O + H_2$	0.041	0.024	0.025
R3: $H + H_2S \rightarrow H_2 + HS$	0.029	0.023	0.025
R4: $H + N_2O \rightarrow OH + N_2$	0.092	0.060	0.082
R5: $H + ClH \rightarrow HCl + H$	0.050	0.023	0.023
R6: $CH_3 + FCl \rightarrow CH_3F + Cl$	0.106	0.063	0.025
R7: $Cl^-\cdots CH_3Cl \rightarrow ClCH_3\cdots Cl^-$	0.020	0.028	0.028
R8: $F^-\cdots CH_3\ Cl \rightarrow FCH_3\cdots Cl^-$	0.024	0.028	0.024
R9: $OH^- + CH_3F \rightarrow HOCH_3 + F^-$	0.032	0.025	0.023
R10: $HN_2 \rightarrow H + N_2$	0.072	0.022	0.064
R11: $H + C_2H_4 \rightarrow CH_3CH_2$	0.096	0.086	0.018
R12: HNC → HCN	0.063	0.052	0.063

Table 9. Mutlireference Diagnostics for Reactions in DBH24 Calculated with *mod*-CPO/MG3S

reaction	saddle point	reactants	products
R1: $OH + CH_4 \rightarrow CH_3 + H_2O$	0.029	0.026	0.024
R2: $H + OH \rightarrow O + H_2$	0.040	0.027	0.024
R3: $H + H_2S \rightarrow H_2 + HS$	0.038	0.033	0.029
R4: $H + N_2O \rightarrow OH + N_2$	0.092	0.060	0.082
R5: $H + ClH \rightarrow HCl + H$	0.051	0.026	0.026
R6: $CH_3 + FCl \rightarrow CH_3F + Cl$	0.077	0.047	0.025
R9: $OH^- + CH_3F \rightarrow HOCH_3 + F^-$	0.036	0.030	0.025
R10: $HN_2 \rightarrow H + N_2$	0.063	0.077	0.061
R11: $H + C_2H_4 \rightarrow CH_3CH_2$	0.096	0.086	0.018
R12: HNC → HCN	0.063	0.052	0.063

Table 10. Mutlireference Diagnostics for Reactions in DBH24 Calculated with *ext*-CPO/MG3S

reaction	saddle point	reactants	products
R1: $OH + CH_4 \rightarrow CH_3 + H_2O$	0.028	0.026	0.025
R2: $H + OH \rightarrow O + H_2$	0.038	0.026	0.024
R3: $H + H_2S \rightarrow H_2 + HS$	0.049	0.043	0.041
R10: $HN_2 \rightarrow H + N_2$	0.070	0.081	0.061
R11: $H + C_2H_4 \rightarrow CH_3CH_2$	0.096	0.086	0.018
R12: HNC → HCN	0.063	0.052	0.063

The comparison to CCSD calculations is interesting from a methodological point of view. Both MRMP2 and CCSD are limited in a formal sense to double excitations, but MRMP2 generates a subset of the triple and higher excitations from the dominant configuration by taking double excitations from other configurations in the CASSCF wave function, and CCSD (a single-reference method) generates all disconnected triple excitations by the coupled-cluster exponential excitation operator. Both methods also generate a subset of quadruple and higher excitations but different subsets. As a consequence of the triple and higher excitations, CCSD should be less sensitive to multireference effects than MP2 (and Tables 5–7 show that it is more accurate for barrier heights), but the present study is the first systematic comparison to MRMP2. Tables 2–4, 6, and 7 show that MRMP2 has an MUE in barrier heights that is a factor of ~1.5 lower than CCSD. This is very welcome because, for systems with a large number N_{atoms} of atoms, the cost of MRMP, like MP, scales as N_{atoms}^5, whereas CCSD scales as $Natoms^6$. We note that using a full-valence active space would cause much worse scaling of MRMP2, but the size of the active spaces does not increase with N_{atoms} for the CPO schemes because they are defined in terms of participating orbitals rather than all valence orbitals. This, in fact, was one of the motivations of defining the CPO schemes the way that we did.

Comparison of Table 2 to Table 5 shows no systematic improvement of MRMP2 over MP2 for the three S_N2 reactions (reactions **R7**-**R9**). The relatively good performance of MP2 for S_N2 reactions is well-known from many previous studies in the literature. Tables 8 and 9 show that S_N2 reactions have smaller than average M values.

It is interesting to center attention on the subset of reactions with larger M values. Reactions **R4**, **R6**, **R10**, and **R12** are the only reactions with $M > 0.04$. Comparing Tables 2, 3, and 5 for these reactions shows especially large errors in MP2 for **R4** and **R10**, which are greatly diminished by MRMP2. However reaction **R6** has large errors by all methods, and reaction **R12** has smaller than average errors for all methods.

Whereas MP2 has a pronounced systematic error, overestimating 21 of the 24 barriers, MRMP2 does not have such a systematic error. Thus one can find a general scaling factor[67,68] for the correlation contribution in MP2, but the optimum general scale factor for MRMP2 is close to unity. In fact, in the notation of the scaling external correlation method,[69] the optimum scale factor F for MRMP2/*nom*-CPO/MG3S is 1.03, and it lowers the MUE by only 0.03 kcal/mol as compared to $F = 1.00$ (no scaling). Hence we do not recommend developing general scaling features for MRMP2.

Next we turn our attention to the comparison of *nom*-CPO, *mod*-CPO, and *ext*-CPO to each other. Table 7 shows no systematic improvement as the size of the active space is improved. While this might be interpreted as a negative result by some, we take this as very encouraging. It shows that a minimal definition of participating orbitals already captures the bulk of the static correlation effect on chemical reaction

Table 11. Saddle Point Geometries (in Å) and Errors for Selected Reactions in DBH24

	geometry			
R2: H + OH → O + H_2	$r_{HH'}$	r_{OH}	$r_{OH'}$	MUE
best est[78]	0.894	1.215	2.109	
MRMP2/*nom*-CPO/MG3S	0.887	1.231	2.118	0.011
MRMP2/*mod*-CPO/MG3S	0.910	1.203	2.113	0.011
MRMP2/*ext*-CPO/MG3S	0.909	1.200	2.109	0.010
MRMP2/*nom*-CPO/aug-cc-pVTZ	0.884	1.239	2.122	0.016
MP2/MG3S	0.859	1.227	2.086	0.054
CCSD/MG3S	0.910	1.190	2.100	0.036
B3LYP/MG3S	0.907	1.202	2.109	0.030
M05−2X/MG3S	0.933	1.167	2.100	0.036
M06−2X/MG3S	0.921	1.179	2.100	0.036
R5: H + ClH → HCl + H	r_{ClH}	$r_{ClH'}$	$r_{HH'}$	MUE
best est[79]	1.480	1.480	2.960	
MRMP2/*nom*-CPO/MG3S	1.482	1.482	2.964	0.003
MRMP2/*mod*-CPO/MG3S	1.490	1.490	2.980	0.013
MRMP2/*nom*-CPO/aug-cc-pVTZ	1.482	1.482	2.964	0.003
MP2/MG3S	1.468	1.468	2.936	0.016
CCSD/MG3S	1.487	1.487	2.975	0.010
B3LYP/MG3S	1.490	1.490	2.979	0.013
M05−2X/MG3S	1.485	1.485	2.969	0.006
M06−2X/MG3S	1.486	1.486	2.973	0.008
R7: $Cl^-\cdots CH_3Cl \rightarrow ClCH_3\cdots Cl^-$	r_{ClC}	$r_{Cl'C}$	$r_{ClCl'}$	MUE
best est[80]	2.305	2.305	4.610	
MRMP2/*nom*-CPO/MG3S	2.302	2.302	4.604	0.004
MRMP2/*nom*-CPO/aug-cc-pVTZ	2.277	2.277	4.553	0.038
MP2/MG3S	2.288	2.288	4.576	0.023
CCSD/MG3S	2.319	2.319	4.637	0.018
B3LYP/MG3S	2.355	2.355	4.710	0.067
M05−2X/MG3S	2.308	2.308	4.616	0.004
M06−2X/MG3S	2.300	2.300	4.600	0.007
R12: HNC → HCN	r_{CH}	r_{NH}	r_{CN}	MUE
best est[81]	1.183	1.387	1.186	
MRMP2/*nom*-CPO/MG3S	1.194	1.379	1.195	0.009
MRMP2/*nom*-CPO/aug-cc-pVTZ	1.193	1.383	1.196	0.008
MP2/MG3S	1.173	1.417	1.186	0.013
CCSD/MG3S	1.179	1.402	1.186	0.006
B3LYP/MG3S	1.190	1.388	1.180	0.005
M05−2X/MG3S	1.177	1.434	1.170	0.023
M06−2X/MG3S	1.172	1.438	1.174	0.025

barrier heights. This means that the MRMP2/*nom*-CPO method is likely to be very useful even for large systems.

We can compare the present method to the MR-G3(MP2) and MR-G3/MP2 model chemistries by Sølling et al.[12] These are multilevel model chemistries; the former is based on MRCI calculations based on full-valence CASSCF, and the latter on CASPT2 (which is essentially the same as MRMP2), again based on full-valence CASSCF. Sølling et al. did not study barrier heights, but for heats of formation they found that the mean unsigned error in the MRCI-based model is 1.2 kcal/mol and that in the CASPT2-based model is 1.6 kcal/mol. The latter may approximately be compared to our mean unsigned errors in reaction energies, which are 1.8−2.6 kcal/mol, depending on the reaction subset, for *nom*-CPO, 2.1−2.2 kcal/mol for *mod*-CPO, and 1.8 kcal/mol for *ext*-CPO. Given the differences in the test data, the results are comparable, although our calculations do not include empirical high-level corrections, whereas the MR-G3(MP2) and MR-G3/MP2 methods each have four empirical parameters. We note that the present methods lead to continuous potential energies, whereas methods with high-level corrections do not.[70,71]

Additionally, we compare MRMP2 to density functional theory. We have shown elsewhere[16] (based on single-point calculations with the MG3S basis set and QCISD/MG3 geometries) that the most popular density functional (B3LYP)[8] has an MUE for the reactions in Table 7 of 4.3 kcal/mol. Table 7 shows that using consistently optimizing geometries reduces this to 4.1 kcal/mol. However one can do better with more recently developed density functionals; for example Table 7 shows that the M06−2X functional[72] leads to an error of only 1.0 kcal/mol. As mentioned above, the *M* diagnostic for the reactions in DBH24 shows that their multireference character is only small (≤0.05) to modest (0.05−0.10) and in one case large (≥0.10). In any event one expects larger errors in both MRMP2 and DFT when *M* gets larger. It would be interesting to test MRMP2 against density functional theory for reactions with larger multireference character such as reactions with biradical transition states, reactions involving coordinately unsaturated transition metals, or reactions of ozone. Such extensions would probably show different trends from those in Table 7, but the extension to transition metals might also require some refinement of the *nom*-, *mod*-, and *ext*-definitions. The mean unsigned error

Table 12. Saddle Point Geometries (in Å) for Some Other Reactions in DBH24

	geometry		
R8: $F^- \cdots CH_3Cl \rightarrow FCH_3 \cdots Cl^-$	r_{FC}	r_{ClC}	r_{FCl}
ref 82	2.030	2.121	4.151
ref 83	2.019	2.124	4.143
MRMP2/*nom*-CPO/MG3S	1.959	2.191	4.150
MP2/MG3S	2.018	2.098	4.116
CCSD/MG3S	2.038	2.114	4.152
B3LYP/MG3S	2.157	2.077	4.234
M05−2X/MG3S	2.051	2.105	4.156
M06−2X/MG3S	2.036	2.096	4.133

	geometry		
R9: $OH^- + CH_3F \rightarrow HOCH_3 + F^-$	r_{OC}	r_{CF}	r_{OF}
ref 83	2.000	1.753	3.753
MRMP2/*nom*-CPO/MG3S	2.045	1.772	3.817
MP2/MG3S	1.981	1.740	3.721
CCSD/MG3S	1.978	1.754	3.732
B3LYP/MG3S	2.051	1.771	3.821
M05−2X/MG3S	1.976	1.742	3.718
M06−2X/MG3S	1.965	1.734	3.699

in the 12 *nom*-CPO/MG3S barrier heights for which the saddle point *M* value is less than 0.05 is 1.3 kcal/mol, and that for the 10 *nom*-CPO/MG3S barrier heights for which the saddle point *M* value is greater than 0.05 is 1.4 kcal/mol, which is essentially the same. For some other methods though, the MUE increases in passing from the M < 0.05 subset to the for the M > 0.05 subset, in particular from 2.5 to 7.5 kcal/mol for MP2, from 2.3 to 2.8 kcal/mol for CCSD, from 1.4 to 2.0 kcal/mol for M05-2X, and from 4.0 to 4.2 kcal/mol for B3LYP (the MUE is 1.0 kcal/mol for both subsets for M06-2X). The more uniform performance of MRMP2 as compared to several other methods is encouraging and is encougaging and supports the hope that MRMP2 might remain accurate for large *M* values, although this clearly needs to be confirmed by actual tests, whereas MP2, CCSD, and hybrid DFT would all be expected to become less accurate in that case.

Table 2 allows us to compare the performance of two basis sets, MG3S and aug-cc-pVTZ; both are augmented or partially augmented with diffuse functions, are multiply polarized, and have triple-split quality for valence orbitals, but aug-cc-pVTZ is much larger (and hence much more expensive). Table 2 shows that aug-cc-pVTZ gives slightly more accurate (on average) reaction energies but significantly less accurate barrier heights. Four of the five reactions (**R3** and **R5** to **R8**) that involve S or Cl have significantly less accurate forward barrier heights with aug-cc-pVTZ than with MG3S. This might be related in part to a known deficiency[73–76] of the aug-cc-pVTZ basis set for 3*p*-block elements that can be remedied by adding tighter *d* functions. To test this possibility we repeated three of the reactions including S or Cl with the aug-cc-pV(T+d)Z basis set, but the barriers did not change by more than 1.0 kcal. This deficiency (i.e., lack of tight *d* functions for 3*p* elements) does not affect the MG3S basis set because MG3S includes the improved 3*d* functions suggested by Curtiss et al.[56] for P, S, and Cl. The present comparison confirms the high efficiency of the MG3S basis set, which we have employed with satisfactory results for a variety of problems in our group.

Finally we consider transition state geometries. It is harder to test theory for transition state geometries than for transition state energetics because so few accurate transition state geometries are known.[77] Table 11 compares the present transition state geometries to accurate results[78–81] for the only four cases in DBH24 for which we judge the best available estimates of the transition state geometries to be accurate (converged with respect to the inclusion of electron correlation energy) to ≤0.005 Å. The reactions in Table 1 all involve making a bond, X-Y, and breaking a bond, Y-Z. In each case we give the three key bond distances, X-Y, Y-Z, and X-Z, where Y-Z is called the donor−acceptor distance. We also give the mean unsigned error of these three distances as compared to the accurate values. Table 11 shows an average MUE (averaged over all four reactions with the MG3S basis set) in transition state bond lengths and donor−acceptor distances of 0.007 Å for MRMP2/*nom*-CPO, 0.018 Å for CCSD, 0.019 Å for M06−2X, and 0.039 Å for MP2 and B3LYP. The decided superiority of MRMP2 is evident but has never been systematically demonstrated in previous work. Extending the active space to *mod*-CPO (two examples) or *ext*-CPO (one example) does not improve the results, but there is little room for improvement.

There are two additional reactions for which reasonably accurate values of transition state geometries have been published.[82,83] We do not believe that the convergence of these geometries to 0.005 Å has been demonstrated, and therefore we did not include them in Table 11, and we do not interpret deviations from the present calculations as necessarily indicating errors in the present calculations, but the comparisons are still interesting and are given in Table 12. The deviations of MRMP2 from the previous calculations are larger than for the reactions in Table 12, and the various results for the $OH^- + CH_3F$ nucleophilic substitution reaction differ greatly (a range of 0.080 Å for the O−C distance and a range of 0.122 Å for the donor−acceptor distance). We conclude that further study of the transition state geometries in Table 12 would be very interesting.

6. Concluding Remarks

We have defined three systematic choices of active space that, unlike full-valence spaces, do not increase in size, for a given reaction type, as the reagents increase in size, and we have tested them with the MRMP2[23,24] wave function method against a database of diverse barrier heights and a smaller database of accurately known transition state geometries. The smallest of the three systematically defined active spaces, called *nom*-CPO, has an average size of only 4.6 active electrons in 4.6 active orbitals for the reactions studied (ranging from 3 active electrons in 3 active orbitals to 11 active electrons in 11 active orbitals), but it captures the bulk of the static correlation energy, which is quite significant for these reactions. Thus the mean unsigned error in barrier heights for MRMP2/*nom*-CPO is 1.4 kcal/mol, whereas single-reference MP2 has a mean unsigned error of 5.0 kcal/mol for the same reactions. Even CCSD, which is well-known to be less sensitive than MP2 to multireference effects, has a mean unsigned error of 2.5 kcal/mol for these reactions. MRMP2 also gives a remarkable improvement in

accuracy for transition state geometries with a mean unsigned error in forming and breaking bond lengths and donor−acceptor distances of only 0.007 Å, as compared to 0.039 Å for MP2 and 0.018 Å for CCSD. The present results confirm earlier indications that MRMP2 can provide accurate barrier heights[84–87] and transition state geometries[44] for chemical reactions. The present work provides systematic demonstration on a diverse set of reactions, and, by defining three levels of active spaces, it paves the way for systematic applications of multireference theoretical model chemistries in the future.

We defined a multireference diagnostic called M that approximately measures the amount of multireference character in the reagents and transition states. It ranges from 0.020 to 0.106 for the reactions in our diverse barrier height database. This establishes a range of validation for the new MRMP2 model chemistries, and further validation is recommended for applications to reactions with $M > 0.1$.

Acknowledgment. This work was supported in part by the United States Department of Energy, Office of Basic Energy Sciences under grant no. DE-FG02-86ER13579.

Supporting Information Available: Optimized molecular geometries in Cartesian coordinates. This material is available free of charge via the Internet at http://pubs.acs.org.

References

(1) Pople, J. A. In *Energy, Structure and Reactivity: Proceedings of the 1972 Boulder Summer Research Conference on Theoretical Chemistry*; Smith, D. W., McRae, W. B., Eds.; Wiley: New York, 1973; p 51.

(2) Pople, J. A. *Rev. Mod. Phys.* **1999**, *71*, 1267.

(3) Head-Gordon, M. *J. Phys. Chem.* **1996**, *100*, 13213.

(4) Zhao, Y.; Truhlar, D. G. *J. Chem. Theory Comput.* **2006**, *2*, 1009.

(5) Pople, J. A.; Radom, L.; Hehre, W. J. *J. Am. Chem. Soc.* **1971**, *93*, 289.

(6) DeFrees, D. J.; Raghavachari, K.; Schlegel, H. B.; Pople, J. A. *J. Am. Chem. Soc.* **1982**, *104*, 5576.

(7) Dewar, M. J. S.; Zoebisch, E. G.; Healy, E. F.; Stewart, J. J. P. *J. Am. Chem. Soc.* **1985**, *107*, 3902.

(8) Stephens, P. J.; Devlin, F. J.; Chabalowski, C. F.; Frisch, M. J. *J. Phys. Chem.* **1994**, *98*, 11623.

(9) Martin, J. M. L. De Oliveira, G. *J. Chem. Phys.* **1999**, *111*, 1843.

(10) Curtiss, L. A.; Raghavachari, K.; Redfern, P. C.; Pople, J. A. *J. Chem. Phys.* **2000**, *112*, 1125.

(11) Lynch, B. J.; Fast, P. L.; Harris, M.; Truhlar, D. G. *J. Phys. Chem. A* **2000**, *104*, 4813.

(12) Sølling, T. I.; Smith, D. M.; Radom, L.; Freitag, M. A.; Gordon, M. S. *J. Chem. Phys.* **2001**, *115*, 8758.

(13) Lynch, B. J.; Zhao, Y.; Truhlar, D. G. *J. Phys. Chem. A* **2005**, *109*, 1643.

(14) Wood, G. P. F.; Radom, L.; Petersson, G. A.; Barnes, E. C.; Frisch, M. J.; Montgomery, J. A. *J. Chem. Phys.* **2006**, *125*, 194106.

(15) Truhlar, D. G. *J. Comput. Chem.* **2007**, *28*, 73.

(16) Zheng, J.; Zhao, Y.; Truhlar, D. G. *J. Chem. Theory Comput.* **2007**, *3*, 569.

(17) Roos, B. O.; Taylor, P. R.; Siegbahn, P. E. M. *Chem. Phys.* **1980**, *48*, 157.

(18) Siegbahn, P. E. M.; Almlöf, J.; Heiberg, A.; Roos, B. O. *J. Chem. Phys.* **1981**, *74*, 2384.

(19) (a) Werner, H.-J.; Knowles, P. J. *J. Chem. Phys.* **1985**, *82*, 5053. (b) Knowles, P. J.; Werner, H.-J. *Chem. Phys. Lett.* **1985**, *115*, 259.

(20) Roos, B. O. *Adv. Chem. Phys.* **1987**, *69*, 399.

(21) Schmidt, M. W.; Gordon, M. S. *Annu. Rev. Phys. Chem.* **1998**, *49*, 233.

(22) (a) Cheung, L. M.; Sundberg, K. R.; Ruedenberg, K. *Int. J. Quantum Chem.* **1979**, *16*, 1103. (b) Ruedenberg, K.; Schmidt, M. W.; Gilbert, M. M.; Elbert, S. T. *Chem. Phys.* **1982**, *71*, 41. FORS was originally defined to denote what whould be labeled a "full-valence" CASSCF calculation in the more popular nomenclature, but it is now generally accepted as being synonymous with CASSCF. See also ref 21.

(23) Hirao, K. *Chem. Phys. Lett.* **1992**, *190*, 374.

(24) Hirao, K. *Int. J. Quantum Chem. Symp.* **1992**, *26*, 517.

(25) Andersson, K.; Malmqvist, P.-Å.; Roos, B. O.; Sadlej, A. J.; Wolinski, K. *J. Phys. Chem.* **1990**, *94*, 5483.

(26) Wolinski, K.; Sellers, H. L.; Pulay, P. *Chem. Phys. Lett.* **1987**, *140*, 225.

(27) Kozlowski, P. M.; Davidson, E. R. *J. Chem. Phys.* **1994**, *100*, 3672.

(28) Brown, F. B.; Shavitt, I.; Shepard, R. *Chem. Phys. Lett.* **1984**, *105*, 363.

(29) Werner, H.-J. *Adv. Chem. Phys.* **1987**, *69*, 1.

(30) Jeziorski, B.; Monkhorst, H. *J. Phys. Rev. A* **1981**, *24*, 1668.

(31) Balkova, A.; Kucharski, S. A.; Meissner, L.; Bartlett, R. J. *J. Chem. Phys.* **1991**, *95*, 4311.

(32) Piecuch, P. Paldus, J. *Theor. Chim. Acta* **1992**, *83*, 69.

(33) Piecuch, P.; Oliphant, N.; Adamowicz, L. *J. Chem. Phys.* **1993**, *99*, 1875.

(34) Balkova, A.; Bartlett, R. J. *J. Chem. Phys.* **1994**, *101*, 8972.

(35) Ghose, K. B.; Piecuch, P.; Adamowicz, L. *J. Chem. Phys.* **1995**, *103*, 9331.

(36) Chattopadhyay, S.; Mahapatra, U. S.; Datta, B.; Mukherjee, B. *Chem. Phys. Lett.* **2002**, *357*, 426.

(37) Pittner, J. *J. Chem. Phys.* **2003**, *118*, 10876.

(38) Li, X.; Paldus, J. *J. Chem. Phys.* **2003**, *119*, 5320.

(39) Li, X.; Paldus, J. *J. Chem. Phys.* **2003**, *119*, 5334.

(40) Eckert-Maksic, M.; Vazdar, M.; Barbatti, M.; Lischka, H.; Maksic, Z. B. *J. Chem. Phys.* **2006**, *125*, 64310.

(41) Li, X.; Paldus, J. *J. Chem. Phys.* **2006**, *125*, 164107.

(42) Li, X.; Paldus, J. *J. Phys. Chem. A* **2007**, *111*, 11189.

(43) Evangelista, F. A.; Allen, W. D.; Schaefer, H. F. *J. Chem. Phys.* **2006**, *125*, 154113.

(44) Ellingson, B. A.; Theis, D. P.; Tishchenko, O.; Zheng, J.; Truhlar, D. G. *J. Phys. Chem. A* **2007**, *111*, 13554.

(45) Gan, Z.; Alexeev, Y.; Gordon, M. S.; Kendall, R. A. *J. Chem. Phys.* **2003**, *119*, 47.

(46) Frenking, G.; Koch, W.; Gauss, J.; Cremer, D. *J. Am. Chem. Soc.* 1988*110*, 8007.

(47) Martin, J. M. L.; Taylor, P. R. *J. Phys. Chem.* **1994**, *98*, 6105.

(48) Hunt, W. J.; Hay, P. J.; Goddard, W. A. *J. Chem. Phys.* **1972**, *57*, 738.

(49) Walch, S. P.; Rohlfing, C. M.; Melius, C. F.; Baushclicher, C. W., Jr. *J. Chem. Phys.* **1988**, *88*, 6273.

(50) Lynch, B. J.; Truhlar, D. G. *J. Phys. Chem. A* **2003**, *107*, 8996.

(51) (a) Herzberg, G. *Spectra of Diatomic Molecules*; 2nd ed.; D. Van Nostrand: Princeton, 1950; pp 540−541, 560−561. (b) Moore, C. National Bureau of Standards (U.S.) Circular 467; 1952. (c) Roberto-Neto, O.; Coitino, E. L.; Truhlar, D. G. *J. Phys. Chem. A* **1998**, *102*, 4568.

(52) Kendall, R. A.; Dunning, T. H., Jr.; Harrison, R. J. J. Chem. Phys. 1992, *96*, 6796.

(53) Woon, D. E.; Dunning, T. H., Jr *J. Chem. Phys.* **1993**, *98*, 1358.

(54) Lynch, B. J.; Zhao, Y.; Truhlar, D. G. *J. Phys. Chem. A* **2003**, *107*, 1384.

(55) Frisch, M. J.; Pople, J. A.; Binkley, J. S. *J. Chem. Phys.* **1984**, *80*, 3265.

(56) Curtiss, L. A.; Raghavachari, K.; Redfern, P. C.; Rassolov, V.; Pople, J. A. *J. Chem. Phys.* **1998**, *109*, 7764.

(57) Zheng, J.; Gour, J. R.; Lutz, J. J.; Wloch, M.; Piecuch, P.; Truhlar, D. G. *J. Chem. Phys.* **2008**, *128*, 44108.

(58) Schmidt, M. W.; Baldridge, K. K.; Boatz, J. A.; Elbert, S. T.; Gordon, M. S.; Jensen, J. H.; Koseki, S.; Matsunaga, N.; Nguyen, K. A.; Su, S. J.; Windus, T. L.; Dupuis, M.; Montgomery, J. A. *J. Comput. Chem.* **1993**, *14*, 1347.

(59) Frisch, M. J.; Trucks, G. W.; Schlegel, H. B.; Scuseria, G. E.; Robb, M. A.; Cheeseman, J. R.; Montgomery, J. A., Jr.; Vreven, T.; Kudin, K. N.; Burant, J. C.; Millam, J. M.; Iyengar, S. S.; Tomasi, J.; Barone, V.; Mennucci, B.; Cossi, M.; Scalmani, G.; Rega, N.; Petersson, G. A.; Nakatsuji, H.; Hada, M.; Ehara, M.; Toyota, K.; Fukuda, R.; Hasegawa, J.; Ishida, M.; Nakajima, T.; Honda, Y.; Kitao, O.; Nakai, H.; Klene, M.; Li, X.; Knox, J. E.; Hratchian, H. P.; Cross, J. B.; Bakken, V.; Adamo, C.; Jaramillo, J.; Gomperts, R.; Stratmann, R. E.; Yazyev, O.; Austin, A. J.; Cammi, R.; Pomelli, C.; Ochterski, J. W.; Ayala, P. Y.; Morokuma, K.; Voth, G. A.; Salvador, P.; Dannenberg, J. J.; Zakrzewski, V. G.; Dapprich, S.; Daniels, A. D.; Strain, M. C.; Farkas, O.; Malick, D. K.; Rabuck, A. D.; Raghavachari, K.; Foresman, J. B.; Ortiz, J. V.; Cui, Q.; Baboul, A. G.; Clifford, S.; Cioslowski, J.; Stefanov, B. B.; Liu, G.; Liashenko, A.; Piskorz, P.; Komaromi, I.; Martin, R. L.; Fox, D. J.; Keith, T.; Al-Laham, M. A.; Peng, C. Y.; Nanayakkara, A.; Challacombe, M.; Gill, P. M. W.; Johnson, B.; Chen, W.; Wong, M. W.; Gonzalez, C.; Pople, J. A. *Gaussian 03, revision C.01*; Gaussian, Inc.: Wallingford, CT, 2004.

(60) Zhao, Y.; Truhlar, D. *MN-GFM - version 3.0*; University of Minnesota: Minneapolis, 2007.

(61) Møller, C.; Plesset, M. S. *Phys. Rev.* **1934**, *46*, 618.

(62) Purvis, G. D., III; Bartlett, R. J. *J. Chem. Phys.* **1982**, *76*, 1910.

(63) Huber, K. P.; Herzberg, G. *Molecular Spectra and Molecular Structure. IV. Constants of Diatomic Molecules*; Van Nostrand Reinhold Co.: New York, 1979.

(64) Herzberg, G., *Electronic spectra and electronic structure of polyatomic molecules*; Van Nostrand: New York, 1966.

(65) (a) Laidig, W. D.; Schaefer, H. F.,., III *J. Chem. Phys.* **1981**, *74*, 3411 (b) Xantheas, S. S.; Atchity, G. C.; Elbert, S. T.; Ruedenberg, K. J. *Chem. Phys.* **1991**, *94*, 8054. (c) Borowski, P.; Andersson, K.; Malmqvist, P.-Å.; Roos, B. O. *J. Chem. Phys.* **1992**, *95*, 2107. (d) Tsueneda, T.; Nakano, H.; Hirao, K. J. *Chem. Phys.* **1995**, *103*, 6520. (e) Szalay, P. G. J. *Phys. Chem.* **1996**, *100*, 6288. (f) Leininger, M. L., III *Chem. Phys.* **1997**, *107*, 9059. (g) Li, X.; Paldus, J. J. *Chem. Phys.* **1999**, *110*, 2844. (h) Vaval, N.; Pal, S. J. *Chem. Phys.* **1999**, *111*, 4051. (i) Xie, D.; Guo, H.; Peterson, K. A. J. *Chem. Phys.* **2000**, *112*, 8378. (j) Ljubic, I.; Sabljic, A. J. *Phys. Chem. A* **2002**, *106*, 4745. (k) Ajitha, D.; Hirao, K.; Pal, S. *Collect. Czech. Chem. Commun.* **2003**, *68*, 47.

(66) Hammond, G. S. *J. Am. Chem. Soc.* **1955**, *77*, 334.

(67) Gordon, M. S.; Truhlar, D. G. *J. Phys. Chem. A* **1986**, *108*, 5412.

(68) Lynch, B. J.; Truhlar, D. G. *J. Phys. Chem. A* **2003**, *107*, 3898.

(69) Brown, F. B.; Truhlar, D. G. *Chem. Phys. Lett.* **1985**, *117*, 307.

(70) Fast, P. L.; Sanchez, M. L.; Corchado, J. C.; Truhlar, D. G. *J. Chem. Phys.* **1999**, *110*, 11679.

(71) Fast, P. L.; Sanchez, M. L.; Truhlar, D. G. *Chem. Phys. Lett.* **1999**, *306*, 407.

(72) Zhao, Y.; Truhlar, D. G. Theor. Chem. Acc., in press; published online athttp://dx.doi.org/10.1007/s00214-007-310-x.

(73) Dunning, T. H.; Petersen, K. A.; Wilson, A. K. *J. Chem. Phys.* **2001**, *114*, 9244.

(74) Wang, N. X.; Wilson, A. K. *J. Phys. Chem. A* **2003**, *107*, 6720.

(75) Wilson, A. K.; Dunning, T. H., Jr. *J. Phys. Chem. A* **2004**, *108*, 3129.

(76) Bell, R. D.; Wilson, A. K. *Chem. Phys. Lett.* **2004**, *394*, 105. Chem. Phys. Lett. 1999, *306*, 407.

(77) Lynch, B. J.; Truhlar, D. G. *J. Phys. Chem. A* **2001**, *105*, 2936.

(78) Bian, W.; Werner, H.-J. *J. Chem. Phys.* **2000**, *112*, 220.

(79) Peterson, K. A.; Dunning, T. H., Jr. *J. Phys. Chem. A* **1997**, *101*, 6280.

(80) Parthiban, S.; Oliveira, G. D.; Martin, J. M. L. *J. Phys. Chem. A* **2001**, *105*, 895.

(81) van Mourik, T.; Harris, G. J.; Polyansky, O. L.; Tennyson, J.; Császár, A.; Knowles, P. *J. Chem. Phys.* **2001**, *115*, 3707.

(82) Botschwina, P.; Horn, M.; Seeger, S.; Oswald, R. *Ber. Bunsenges. Phys. Chem.* **1997**, *101*, 387.

(83) Gonzales, J. M.; Pak, C.; Cox, R. S.; Allen, W. D.; Schaefer, H. F.; Császár, A. G.; Tarczay, G. *Chem. Eur. J.* **2003**, *9*, 2173.

(84) Roberto-Neto, O.; Machado, F. B. C.; Truhlar, D. G. *J. Chem. Phys.* **1999**, *111*, 10046.

(85) Kobayashi, Y.; Kamiya, M.; Hirao, K. *Chem. Phys. Lett.* **2000**, *319*, 695.

(86) Tishchenko, O.; Vinckier, C.; Nguyen, M. T. *J. Chem. Phys. A* **2004**, *108*, 1268.

(87) Tishchenko, O.; Vinckier, C.; Ceulemans, A.; Nguyen, M. T. *J. Chem. Phys. A* **2005**, *109*, 6099.

CT800077R